The Canadian Mineralogist
Vol. 38, pp. 525-543(2000)

REDISTRIBUTION OF MAJOR AND TRACE ELEMENTS DURING THE FORMATION OF BIOTITE–PLAGIOCLASE REACTION ZONES AT BOUNDARIES BETWEEN AMPHIBOLITE AND K-FELDSPAR GNEISS, OTTER LAKE AREA, QUEBEC, CANADA

RALPH KRETZ

Ottawa–Carleton Geoscience Centre, Department of Earth Sciences, University of Ottawa, Ottawa, Ontario K1N 6N5, Canada

ABSTRACT

In the Otter Lake area of Quebec, in the southern Grenville Province of the Canadian Shield, mineral zones a few cm wide occur at boundaries between deformed sheets of amphibolite and the enclosing K-feldspar gneiss. The zones consist of a biotite-rich subzone (free of hornblende) adjacent to amphibolite, and one with abundant plagioclase (free of K-feldspar) adjacent to gneiss. Thus biotite and plagioclase evidently crystallized at the expense of hornblende and K-feldspar. Referring to amphibolite as A, the entire reaction-zone as B, and gneiss as C, then for any element that was locally conserved,

$$a' = \frac{fd^{\mathrm{B}}w^{\mathrm{B}} - d^{\mathrm{C}}w^{\mathrm{C}}}{d^{\mathrm{A}}w^{\mathrm{A}} - d^{\mathrm{C}}w^{\mathrm{C}}}$$

where *d* stands for rock density, *w* for weight fraction of the element, and *f* for fractional change in volume; the variable *a*' locates the original amphibolite–gneiss interface, being the distance from that interface to the present interface between the reaction zone and amphibolite, divided by the width of the reaction zone. Applying this equation to 24 major and trace elements, assuming little or no change in volume (*f* = 1.0) leads to the conclusion that 1) the original amphibolite–gneiss interface was located at the present boundary between the biotite-rich and plagioclase-rich subzones, and 2) in two samples, all of the elements except Cs (gained) and Ca, K, and Ba (lost) were locally conserved. Reaction equations, *e.g.*, 0.65 hornblende + 0.86 K-feldspar → 1.0 biotite + 0.32 albite + 0.25 anorthite + 2.5 quartz (sample 1), are nearly balanced, except for Ca. In addition, the reaction produced gradients in the composition of biotite ($0.58 < X_{\mathrm{Mg}} < 0.48$) and plagioclase ($0.40 < X_{\mathrm{an}} < 0.21$) within the subzone adjacent to gneiss; such gradients can be described by use of diffusion equations. Crystals of garnet, where present, remained passive except that some Ca and Mg entered their margins, in exchange for Fe, resulting in a close approach to Mg–Fe exchange equilibrium with associated crystals of biotite. As reaction progressed, most elements remained in place, in the sense that atoms released from hornblende entered nearby crystallizing biotite; only Ca and Na were displaced across the entire reaction-zones toward gneiss, and K, Ba, and Rb in the opposite direction. Atomic re-arrangements evidently occurred by both within-crystal and crystal-boundary diffusion.

Keywords: reaction zones, amphibolite, K-feldspar gneiss, major elements, trace elements, conservation, exchange equilibrium, diffusion, strain energy, Otter Lake, Grenville Province, Quebec.

SOMMAIRE

Dans la région du lac Otter, province de Québec, dans le secteur sud de la Province du Grenville du Bouclier Canadien, des zones centrimétriques de minéraux néoformés marquent l’interface entre des niveaux déformés d’amphibolite et les roches gneissiques à feldspath potassique qui les renferment. Dans ces zones de réaction, on distingue une sous-zone riche en biotite, dépourvue de hornblende et voisine de l’amphibolite, et une autre riche en plagioclase, dépourvue de feldspath potassique et voisine de l’encaissant gneissique. C’est donc dire que biotite et plagioclase ont de toute évidence cristallisé aux dépens de hornblende et feldspath potassique. Si on considère l’amphibolite comme le domaine A, la zone de réaction entière comme B, et le gneiss comme C, la relation suivante s’applique pour tout élément conservé à courte échelle:

$$a' = \frac{fd^{\mathrm{B}}w^{\mathrm{B}} - d^{\mathrm{C}}w^{\mathrm{C}}}{d^{\mathrm{A}}w^{\mathrm{A}} - d^{\mathrm{C}}w^{\mathrm{C}}}$$

Ici, *d* représente la densité de la roche, *w* est la fraction pondérale de l’élément, et *f* représente le changement fractionnel du volume. Le quantité variable *a*' situe l’interface originel entre l’amphibolite et le gneiss, étant la distance entre cet interface et l’interface actuelle entre la zone de réaction et l’amphibolite, divisée par la largeur de la zone de réaction. L’application de cette équation à 24 éléments majeurs et traces, en supposant un changement de volume très faible ou nul (*f* = 1.0), mène aux conclusions que 1) l’interface amphibolite–gneiss originelle était située au même endroit que l’interface entre les sous-zones à biotite et à plagioclase, et 2) dans deux échantillons, tous les éléments sauf le Cs (qui a augmenté) et le Ca, K, et Ba (perdus) ont été conservés à l’échelle locale. Les équations qui rendent compte de la réaction, par exemple 0.65 hornblende + 0.86 feldspath potassique → 1.0 biotite + 0.32 albite + 0.25 anorthite + 2.5 quartz, sont presque balancées, sauf pour le Ca. De plus, les réactions ont produit des gradients en composition de la biotite ($0.58 < X_{\mathrm{Mg}} < 0.48$) et du plagioclase ($0.40 < X_{\mathrm{an}} < 0.21$) à l’intérieur de la sous-zone adjacente au gneiss; on peut décrire de tels gradients avec des équations prévues pour expliquer la diffusion. Les cristaux de grenat, où ils sont présents, sont demeurés passifs à l'exception d'un peu de Ca et de Mg, qui ont pénétré les bordures en échange pour le Fe, assurant ainsi un équilibre d'échange Mg–Fe avec les cristaux associés de biotite. A mesure que la réaction progressa, la plupart des éléments sont restés sur place, dans le sens que les atomes libérés de la hornblende sont incorporés dans la biotite avoisinante. Seuls Ca et Na ont été déplacés d'une zone à l'autre vers le gneiss, et le K, Ba, et Rb ont migré dans la direction opposée. Les réorganisations d'atomes ont impliqué à la fois diffusion intracristalline et diffiusion à la bordure des cristaux.

(Traduit par la Rédaction)

Mots-clés: zones de réaction, amphibolite, gneiss à feldspath potassique, éléments majeurs, éléments traces, conservation, équilibre d'échange, diffusion, énergie de d.formation, lac Otter, Province du Grenville, Quebec.

INTRODUCTION

Mineral zones less than 1 cm to several cm wide are commonly present at boundaries between bodies of metamorphic rock of different chemical composition. Most conspicuous are zones of clinopyroxene at boundaries between marble and silicate rock, but mineral zones with abundant biotite and other minerals also occur where layers of amphibolite were once in contact with felsic schist, gneiss, or granulite.

All reaction zones are of interest because both products and reactants are available for study. In many small-scale reaction-zones, reactant crystals initially in contact (*e.g.*, olivine and plagioclase) became increasingly separated as reaction progressed, but normally by distances of only a mm or less. By comparison, in zones that formed between different rock-types, crystals evidently continued to react with each other even after they became separated by several cm. These findings provide information on atomic mobility in metamorphic terranes.

In the Otter Lake area, Quebec, in the southern part of the Grenville Province, mineral zones with abundant biotite and plagioclase are commonly present at boundaries between layers of amphibolite and the enclosing K-feldspar gneiss. Reaction zones of this kind were examined in detail by Ono (1977; Ryoke, Japan), Tuisku (1992; Honkaniemi, Finland) and Owen (1993; Port-aux-Basques, Newfoundland). In these studies, difficulties were encountered in locating the original amphibolite – felsic rock interface, and therefore in identifying, with confidence, those elements that were added to or lost from the reaction zones.

A principal aim of the present study is to derive a new equation that will permit one to estimate, by use of the compositions of all three units (amphibolite, reaction zone, gneiss) the location of the original amphibolite–gneiss interface, and to identify elements that were gained or lost, taking into consideration differences in rock density and a change in volume. Note that the problem is not one of simply comparing altered and unaltered volumes of rock, which can be dealt with by use of the well-known Gresens (1967) equation. Secondly, by use of mineral compositions, an attempt will be made to construct equations for the entire hornblende + K-feldspar → biotite + plagioclase reaction, and for the half reactions that occurred on either side of a given zone. Finally, an explanation will be sought for the striking non-homogeneous distribution of minerals and of major and trace elements within the reaction zones.

GEOLOGICAL CONTEXT

Study samples were collected from the Otter Lake area, centered 70 km northwest of Ottawa, where bodies of metasedimentary, metavolcanic, and plutonic rock were highly deformed under conditions of the upper amphibolite facies and, locally, to the lower granulite facies. The various metamorphic rocks have been grouped as follows: 1) marble and skarn (Kretz 1980, 1988), 2) plagioclase gneiss and amphibolite (with calcic clinopyroxene, hornblende, biotite, garnet, sillimanite), including minor quartzite and granulite (Kretz 1978, 1990), 3) metagabbro and minor meta-peridotite (Kretz *et al.* 1989), 4) K-feldspar gneiss, mainly veined gneiss with local garnet and rare sillimanite (Kretz 1994a), and 5) various granitic and syenitic rocks.

The principal tectonic-metamorphic event that affected the above lithologic units occurred between 1250 and 1190 Ma (Rivers 1997); in the study area, estimates of the temperature and pressure of this event are 7×10^2°C and 7 kbar (7×10^2 MPa) (Kretz 1997), and these conditions presumably existed approximately during formation of the reaction zones to be described here.

STUDY SAMPLES

Two samples of reaction zones were taken from the Otter complex, which consists mainly of veined gneiss (group 4) as well as layers of plagioclase gneiss and amphibolite (group 2). Sample 1 is from the boundary between K-feldspar gneiss and a conformable layer of amphibolite, 5 cm wide, located 15.7 km southwest of Otter Lake village (45°47.55' N, 76°37.0' W; site 5 of Kretz 1994a), whereas Sample 2 (Figs. 1, 2) is from a road cut in Highway 301, 13.8 km northeast of Otter Lake village (stop 3 of Kretz 1997). An additional

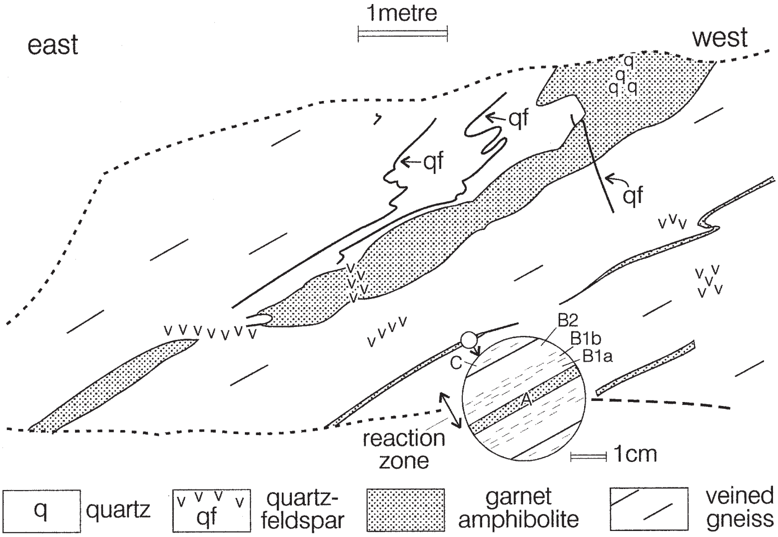

FIG. 1. Geological setting, Sample 2.

sample (number 3), very similar to Sample 2 and from the same location, is used to provide additional information where needed.

In the present report, symbol A refers to amphibolite, B to the reaction zone, and C to gneiss. In Sample 1, B can be divided into B1 (adjacent to amphibolite) which is rich in biotite, and B2 (adjacent to gneiss) with abundant plagioclase. In sample 2, which contains garnet, B1 can be further divided into B1a and B1b (Fig. 2). Mineral assemblages and proportions in these zones are presented in Tables 1 and 2, and in Figure 3; microstructural information is compiled in Table 3. In addition to the minerals listed in Tables 1 and 2, minor retrograde muscovite (an alteration of plagioclase) is

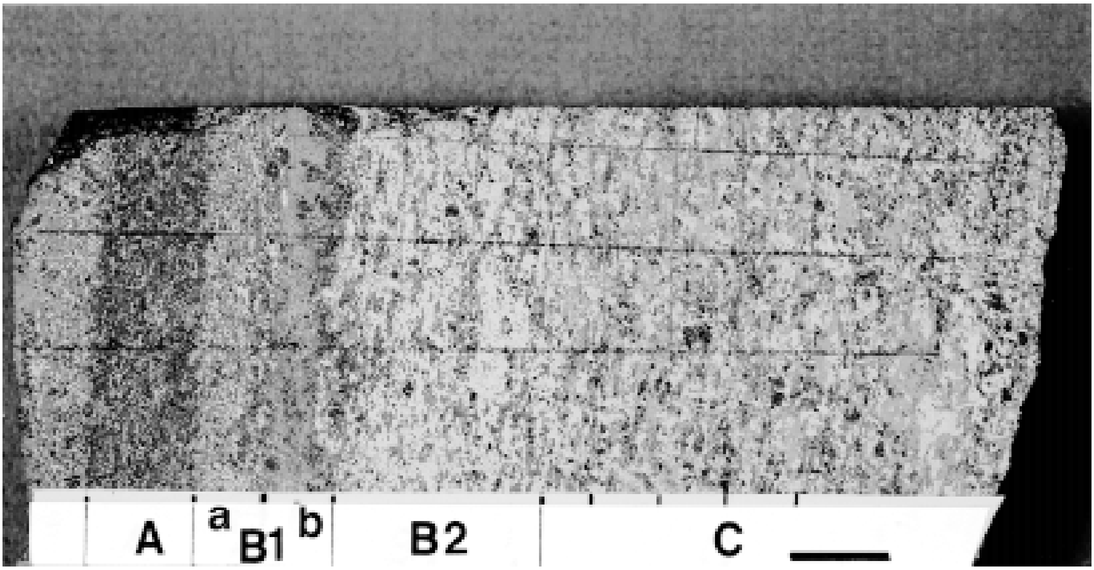

FIG. 2. Sample 2, stained surface (yellow: K-feldspar), A: amphibolite, C: K-feldspar gneiss, B: reaction zone, which in this sample is divided into B1a, B1b, and B2. Ticks above letter C are boundaries to slices that were analyzed separately. Bar: 1 cm.

TABLE 1. MINERAL PROPORTIONS, SAMPLE 1

	A	+/-	B	+/-	C	+/-	B1	+/-	B2	+/-
Quartz/vol%	0.0		24.4	1.5	27.9	2.1	8.0	1.9	29.0	1.8
Plagioclase	25.0	4.0	51.2	1.7	44.2	2.3	30.0	3.1	55.4	2.0
K feldspar	0.0		<1.0		18.2	1.8	0.0		<1.0	
Biotite	5.2	2.1	20.8	1.4	9.3	1.4	53.0	3.4	14.4	1.4
Hornblende	64.4	4.5	0.0		0.0		0.0		0.0	
Titanite	<0.5		0.0		0.0		<0.5		0.0	
Apatite	<0.1		<1.0		<1.0		<1.0		<1.0	
Magnetite	~0.5		<0.5		<0.5		<0.5		<0.5	
Ilmenite*	~4.0	1.8	~1.4	0.4	~0.5		~6.0	1.6	~0.5	
Fe sulfide	~0.5		<0.5		0.0		~0.5		<0.5	
Density/g cm^{-3}	3.07		2.76		2.70		2.96		2.72	
Width/mm	46.0		43.1		>12		7.9		35.2	
Modal points	464		3522		1854		875		2647	

* Ilmenite in A and B1, with inclusions of rutile
+/-: 0.95 confidence limits

present in A and B1a of Sample 2, and very minor epidote, actinolite and chlorite, as clusters in Sample 1.

From field observations, particularly at and near the site where Sample 2 was obtained, amphibolite layers have been deformed to fold, pinch-and-swell, and boudinage structures (Fig. 1), and the amphibolite obviously formed relatively rigid bodies. The strong biotite foliation in zone B1 (Table 3) is interpreted as an expression of a high concentration of strain at amphibolite–gneiss boundaries, implying that the reaction zones formed prior to or during deformation of the amphibolite layers.

METHODS

Mineral proportions were determined by the point-count procedure applied to thin sections and stained surfaces. Following Chayes (1956), 0.95 confidence limits to these estimates were calculated by use of the equation

$$\pm 1.96\, s = \pm 1.96\, [p(1-p)/N]^{1/2} \qquad (1)$$

where s is an estimate of standard deviation, p is the number of points falling on a given mineral, and N is the total number of points counted.

The density of rock fragments (A, B, C) was measured by the standard method of weighing them in water and air.

The rock samples were analyzed using fused discs and a Philips PW2400 X-ray fluorescence (XRF) spectrometer at the University of Ottawa; the concentration of additional trace elements (Sc, Co, Zn, Cs, La, Ce) was determined by instrumental neutron-activation analysis (INAA) at Activation Laboratories, Ancaster, Ontario. The Wilson method was used to determine FeO. A rough estimate of H_2O content was calculated from hornblende and biotite formulas and modal proportions.

The precision of XRF results in our laboratory can be expressed by use of the equation

$$\pm 1.96\, s = \pm 1.96\, \mathrm{k}c^{2/3}, \qquad (2)$$

where c is concentration (wt% oxide, major elements; ppm element, trace elements) and k = 0.002 (Mn), 0.0046 (Si, Ti, Al, Fe, Mg, Ca, K), 0.010 (Na), 0.029 (Sr), 0.071 (V, Cr, Y, Zr) and 0.15 (P, Ni, Rb) (Kretz & Hartree 1998). For the INAA data, an estimate of precision, based on the repeated (n = 10) analysis of a sample of hornblende, is

$$\pm 1.96\, s = \pm 1.96\, \mathrm{k}c/100, \qquad (3)$$

with k = 1.1 (Sc, La), 3.2 (Ce) and 5 (Cs, Co, Zn) (Kretz *et al.* 1999).

TABLE 2. MINERAL PROPORTIONS, SAMPLE 2

	A	+/-	B	+/-	C	+/-	B1a	+/-	B1b	+/-	B2	+/-
Quartz/vol%	13.5	2.1	29.8	1.4	26.0	1.4	25.7	3.7	20.4	2.6	33.2	1.8
Plagioclase	11.6*	2.1	41.8	1.5	31.7	1.5	32.1	3.7	5.3	1.4	53.3	1.9
K feldspar	0.0		0.0		31.3	1.5	0.0		0.0		0.0	
Garnet	4.8	1.3	7.0	0.8	1.8	0.4	9.1	2.3	24.1	2.7	2.3	0.6
Biotite	5.1	1.4	19.1	1.2	8.7	0.9	27.2	3.5	45.8	3.2	10.4	1.2
Hornblende	58.5	3.1	0.0		0.0		0.0		0.0		0.0	
Zircon	<0.1		<0.1		<0.1		<0.1		<0.1		<0.1	
Apatite	<0.5		<0.5		<0.5		<0.5		0.5		<0.5	
Magnetite	1.0	0.6	0.1		0.0		0.3		0.2		0.0	
Ilmenite**	5.1	1.4	1.7	0.4	0.3		5.0	1.7	3.6	1.2	0.3	
Fe sulfide	0.3		0.1		0.03		0.3		0.1		0.02	
Density/g cm^{-3}	3.19		2.85		2.70		2.98		3.14		2.77	
Width/mm	10		33		>32		6.5		5.5		21	
Modal points	1040		4470		4300		640		1000		2830	

* Includes muscovite alteration
** With inclusions of rutile
+/-: 0.95 confidence limits

TABLE 3. MICROSTRUCTURAL DATA, SAMPLES 1 AND 2

		Crystal shape	Crystal size*	Crystal orientation	Crystal distribution
1	A	Hbl slightly elongate, anhedral; Bt thin tabular; Pl, Ilm, equidimensional anhedral	Hbl, Bt 2 mm; Pl, Ilm 0.5 mm	Strong foliation (Hbl, Bt)	Uniform
	B1	Bt tabular; Pl, Qtz, Ilm equidimensional anhedral	Bt 2 mm; Pl, Qtz 0.5 mm; Ilm 0.4 mm	Intense foliation (Bt)	Slightly non-uniform (gneissic)
	B2	Bt tabular; Pl, Qtz, Ilm equidimensional anhedral	Bt, Pl, Qtz, Ilm 1.0 mm	Strong foliation (Bt)	Uniform
	C	Bt tabular; Pl, Kfs, Qtz equidimensional to slightly elongate	Bt 1 mm; Pl, Qtz 2 mm; Kfs 0.6 mm	Strong foliation (Bt, ribbon Qtz); foliation in all zones parallel to contacts	Bt clusters (gneissic)
2	A	Hbl elongate, anhedral; Bt tabular; Grt, Pl, Qtz, Ilm equidimensional anhedral	Hbl, Grt, Bt 1.5 mm; Pl, Qtz, Ilm 0.3 mm	Moderate foliation (Hbl); weak foliation (Bt)	Uniform; many inclusions of Ilm, Qtz, Pl in Grt
	B1a	Bt tabular; Grt, Pl, Qtz, Ilm equidimensional anhedral	Grt 2 mm; Pl 1.5 mm; Pl, Qtz, Ilm 0.3 mm	Strong foliation (Bt)	Uniform; many inclusions in Grt, as in A
	B1b	As in B1a	As in B1a	Intense foliation (Bt); some bent Bt crystals	Uniform; some Grt crystals with inclusions as in A, others nearly free of inclusions
	B2	Bt tabular; Qtz elongate; Grt, Pl, Ilm equidimensional anhedral	Grt 4 mm; Qtz 3 mm; Pl 1.0 mm; Bt 0.5 mm	Strong foliation (Bt, Qtz)	Uniform to slightly gneissic (Bt clusters); few inclusions in Grt
	C	Bt tabular; Qtz elongate; Grt, Pl, Qtz, Ilm equidimensional anhedral	Grt, Qtz 2 mm; Pl, Kfs 1.5 mm	Strong foliation (Bt, Qtz)	As in B2

* maximum dimension, largest crystals
Symbols: Hbl hornblende, Bt biotite, Grt garnet, Pl plagioclase, Kfs K feldspar, Qtz quartz, Ilm ilmenite.

Confirmation of a high level of accuracy in the XRF results was obtained by re-analyzing portions of Sample 2 (A, B1a, B1b, three slices of B2 and four of C) by the ICP (inductively coupled plasma) method (Bondar-Clegg, Ottawa) and in the case of the INAA results, by submitting to the laboratory a masked sample of an international standard.

Minerals were analyzed at the McGill University Electron Microprobe Laboratory, by use of a CAMEBAX instrument, operating under the following conditions: accelerating voltage 15.0 kV, current 8 nA (hornblende, biotite, feldspar) and 10 nA (garnet), counting time 25 s, beam width 5 μm, and with natural minerals as standards.

The following relation from Potts *et al.* (1983) provides an estimate of the precision of the electron-microprobe results:

$$\pm 1.96\, s = \pm 1.96\, [0.04\, c^{1/2}]. \qquad (4)$$

In examining variation in the composition of biotite within the samples selected for study, *local* variation within an area 2.0 × 0.5 mm near the B2–C boundary in Sample 1 (two determinations on each of five crystals) was used as a measure of uncertainty. The results, expressed as 100*s*/mean, are SiO_2 0.56, Al_2O_3 2.44, TiO_2 5.52, FeO_T 3.49, MgO 1.99, MnO 18.3, K_2O 1.10, Na_2O 31.4, F 7.6, and Cl 6.2. As expected, the standard deviations implied by these numbers are similar to or slightly greater than those calculated by use of equation (4). This local variation in MgO, TiO_2, and F is used to construct error bars in Figure 7 (below) and as an aid in defining error bars for plagioclase in the same figure.

The FeO content of minerals was determined by titration (Wilson method) on hornblende separated from amphibolite in Samples 1 and 2, and on biotite separated from zones B1 and B2 in Sample 1 and from B1b, B2, and C in Sample 2; the ferrous/(total iron) ratios so obtained were then applied to biotite crystals in zones from which this mineral was not separated. Formula calculations for garnet indicate that all or nearly all Fe is ferrous iron.

RESULTS

Mineral proportions and rock densities are presented in Tables 1 and 2, and the chemical (bulk)

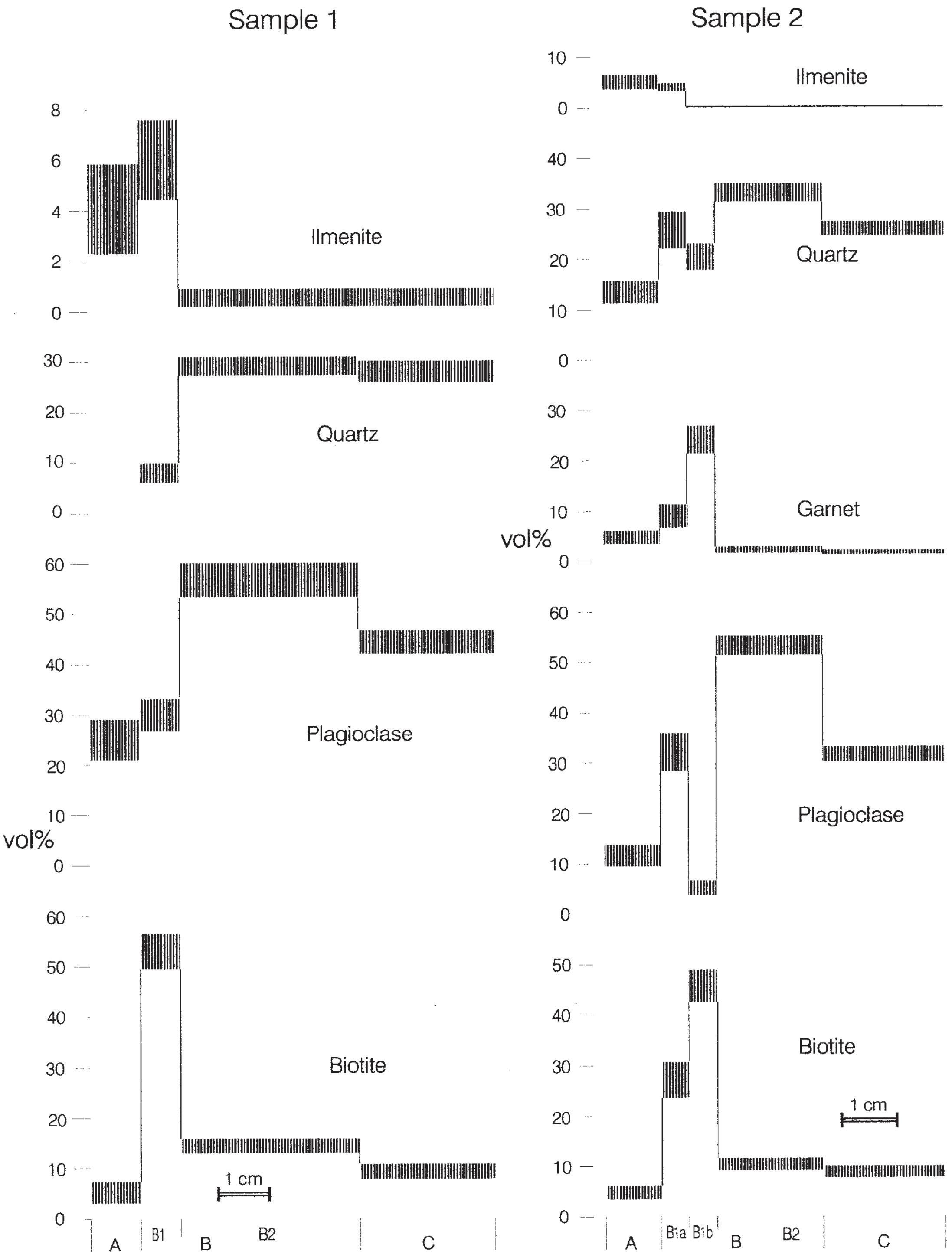

FIG. 3. Mineral proportions in Samples 1 and 2, data from Tables 1 and 2. Uncertainty (0.95 confidence) in the modal analyses is indicated.

TABLE 4. CHEMICAL COMPOSITION, SAMPLE 1

	A	B	C	B1	B2
SiO_2/wt%	47.2	64.9	67.7	51.9	67.5
TiO_2	2.37	0.98	0.69	2.29	0.72
Al_2O_3	14.2	15.0	14.8	13.9	15.2
Fe_2O_3	5.3	2.4	1.44	5.6	1.73
FeO	9.35	4.21	3.15	9.29	3.19
MnO	0.23	0.074	0.056	0.160	0.057
MgO	6.36	2.31	1.50	5.60	1.64
CaO	9.22	3.07	1.86	2.75	3.13
Na_2O	2.36	3.65	3.70	1.71	4.04
K_2O	1.18	2.25	3.97	4.38	1.82
H_2O	1.6	0.89	0.40	2.3	0.62
P/ppm	1390	722	580	1430	580
Sc	47.0	13.0	9.9	25.7	10.4
V	370	126	71	355	81
Cr	122	51	31	134	35
Co	67	54	55	64	52
Ni	64	29	24	63	23
Zn	221	174	124	273	154
Rb	27	118	119	251	91
Sr	151	241	258	116	267
Y	51	32	34	19	35
Zr	179	275	271	200	291
Cs	0.8	4.4	3.3	10.4	3.2
Ba	143	427	980	660	380
La	12.3	29.0	30.5	17.4	31.3
Ce	37	61	63	38	66

TABLE 5. CHEMICAL COMPOSITION, SAMPLE 2

	A	B	C	B1a	B1b	B2
SiO_2/wt%	45.7	62.8	69.1	52.7	42.1	70.0
TiO_2	3.35	1.39	0.55	3.99	3.37	0.55
Al_2O_3	13.2	14.5	14.8	15.1	15.1	14.7
Fe_2O_3	8.9	3.5	0.99	7.6	7.7	2.2
FeO	9.5	5.3	2.9	6.3	12.3	2.1
MnO	0.24	0.154	0.037	0.16	0.33	0.10
MgO	6.37	2.70	0.80	3.35	7.28	0.81
CaO	8.21	3.56	1.94	2.95	2.88	3.97
Na_2O	0.77	1.83	3.01	0.21	0.09	3.60
K_2O	1.53	2.44	4.67	4.31	5.60	1.34
H_2O	1.5	0.82	0.37	1.2	2.0	0.45
P/ppm	1550	1130	894	1940	1730	826
Sc	51	21	9	25	44	14
V	509	180	37	508	490	61
Cr	131	54	16	135	118	19
Co	55	41	32	59	56	32
Ni	78	56	16	69	68	21
Zn	408	230	132	335	429	153
Rb	47	146	163	237	339	83
Sr	47	98	157	79	30	125
Y	78	54	44	39	71	51
Zr	214	315	353	267	260	309
Cs	1.2	7.4	4.6	8.8	18.6	4.2
Ba	351	370	1090	1030	600	246
La	12	33	56	22	24	39
Ce	52	76	93	53	55	87

compositions, in Tables 4 and 5. Results of electron-microprobe analyses of hornblende and K-feldspar, and selected results for biotite and plagioclase (and garnet in Sample 2) are compiled in Tables 6 and 7. More detailed information on the composition of biotite, plagioclase, and garnet is presented in the figures to follow.

TABLE 6. MINERAL COMPOSITIONS, SAMPLE 1
BIOTITE–PLAGIOCLASE REACTION ZONES,
OTTER LAKE, QUEBEC

	Hornblende	Biotite					
Zone:	A	A	B1	B2			C
SiO_2 /wt%	42.1	36.3	36.6	36.1	35.8	35.7	35.4
Al_2O_3	11.60	15.2	15.5	15.1	15.0	15.6	16.2
TiO_2	1.08	3.10	3.32	4.00	4.31	4.20	4.30
Fe_2O_3	6.4	1.82	1.82	2.98	2.98	2.98	2.98
FeO	11.9	15.9	15.4	16.2	16.8	17.0	16.8
MgO	9.37	12.6	12.3	11.1	10.0	9.1	8.6
MnO	0.40	0.18	0.24	0.26	0.30	0.33	0.27
CaO	11.55	0.0	0.0	0.0	0.0	0.0	0.0
Na_2O	1.40	0.038	0.032	0.044	0.036	0.050	0.054
K_2O	1.31	10.2	10.4	10.1	10.2	10.3	10.4
F	0.31	0.64	0.57	0.51	0.44	0.38	0.34
Cl	0.20	0.20	0.18	0.18	0.17	0.19	0.20
X_{Mg}	0.58	0.59	0.59	0.55	0.52	0.49	0.48

	Plagioclase						K feldspar
Zone:	A	B1	B2			C	C
SiO_2	58.5	59.0	60.3	62.4	63.3	63.9	65.2
Al_2O_3	26.5	26.2	25.5	24.4	23.3	23.2	18.4
Fe_2O_3	0.118	0.139	0.063	0.064	0.055	0.043	0.015
CaO	8.43	8.22	7.41	5.92	4.79	4.38	0.00
Na_2O	6.7	6.86	7.24	8.04	8.66	8.96	0.735
K_2O	0.133	0.168	0.191	0.249	0.295	0.264	16.64
X_{an}	0.41	0.40	0.36	0.29	0.23	0.21	
X_{or}							0.94

GAINS AND LOSSES: THE CONSERVATION PROBLEM

It is apparent from Tables 4 and 5 that for nearly all of the elements listed, concentrations in the entire reaction-zone (B) of each study sample are intermediate to those in amphibolite (A) and gneiss (C), as would be expected if these elements were locally conserved. The position of the original A–C interface and the question of whether atoms of any elements were added or removed during reaction-zone formation can be examined by use of an equation that takes into consideration differences in density among A, B, and C, and the possibility that a change in volume has occurred at B. This equation is now derived.

Ideally, one may view a reaction zone (volume B in Fig. 4) at the boundary of two bodies of rock (A and C) as the result of a transformation of a portion of A, labeled A', and a portion of C, labeled C'. We wish to determine if this transformation occurred with or without the addition of atoms of one or more elements from beyond the reaction zone.

Suppose that the original A–C interface was located a distance *a* cm from the present A–B interface and *c* cm from the present B–C interface (Fig. 4). The volume of B, as presently observed, is first normalized to 1.0 cm^3 by introducing *a*' and *c*', defined as *a*/(*a* + *c*) and *c*/(*a* + *c*) respectively, *i.e.*, *a*' + *c*' = 1.0. Furthermore, let

TABLE 7. MINERAL COMPOSITIONS, SAMPLE 2
BIOTITE–PLAGIOCLASE REACTION ZONES,
OTTER LAKE, QUEBEC

	Hornblende	Biotite					
Zone:	A	A	B1a	B1b	B2	C	C
SiO_2/wt%	41.8	36.9	36.3	36.2	35.0	34.3	
Al_2O_3	13.0	15.0	15.7	15.9	16.0	17.4	
TiO_2	0.89	3.0	2.3	3.2	3.9	4.4	
Fe_2O_3	5.08	2.7	2.8	2.9	3.3	3.7	
FeO	13.9	14.7	15.5	15.9	18.7	20.3	
MgO	9.27	14.0	12.6	12.0	9.3	6.4	
MnO	0.14	0.03	0.04	0.04	0.04	0.03	
CaO	11.3	0.0	0.0	0.00	0.01	0.01	
Na_2O	1.33	0.07	0.06	0.06	0.05	0.07	
K_2O	1.16	10.4	10.3	10.4	10.3	10.2	
F	0.45	1.2	0.9	0.9	0.7	0.4	
Cl	0.20	0.19	0.22	0.19	0.19	0.11	
X_{Mg}	0.54	0.63	0.59	0.57	0.47	0.36	
		Garnet margins					
crystal/spot		1/4	4/12	7/19	12/33	21/49	
[Fe]		66.0	66.1	68.4	78.6	82.9	
[Mg]		15.1	15.5	14.2	13.2	11.0	
[Mn]		3.6	3.6	3.7	2.5	2.6	
[Ca]		15.3	14.8	13.7	5.7	3.50	
X_{Mg}		0.186	0.190	0.172	0.144	0.117	
		Plagioclase					K-feldspar
SiO_2		45.9	45.9	46.1	54.5	62.8	64.7
Al_2O_3		33.9	33.5	33.8	28.2	23.7	18.5
Fe_2O_3		0.29	0.19	0.20	0.10	0.01	0.02
CaO		17.7	17.6	17.3	10.3	5.0	0.04
Na_2O		1.34	1.58	1.75	5.3	8.7	1.40
K_2O		0.018	0.051	0.043	0.15	0.26	15.53
X_{an}		0.88	0.86	0.84	0.52	0.24	
X_{or}							0.88

d^A, d^B, d^C = density (g/cm^3) of A, B, C
w^A, w^B, w^C = weight fraction of a specified element in volumes, A, B, C
$d^A\, w^A\, a'$ = grams of the specified element in volume A', prior to transformation
$d^C\, w^C\, c'$ = grams of the specified element in volume C', prior to transformation
(Note that the concentration of an element in A' and C' can only be estimated by determining concentrations in A and C, immediately adjacent to B)
$d^B\, w^B\, (a' + c')$ = measured grams of the specified element in volume B
f = fractional change in volume at B [= final volume (B) / initial volume (A' + C')]

Now for each element that is locally conserved,

$$d^A\, w^A\, a' + d^C w^C c' = f\,[d^B w^B\, (a' + c')], \tag{5}$$

and by rearrangement of terms, recalling that $a' + c' = 1.0$,

$$a' = \frac{f d^B w^B - d^C w^C}{d^A w^A - d^C w^C} \tag{6}$$

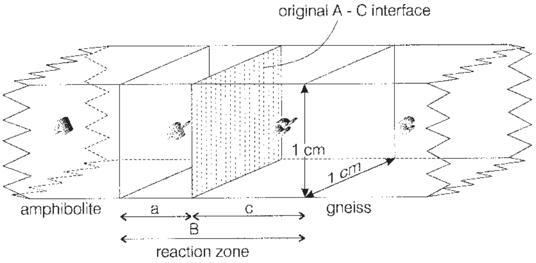

FIG. 4. Idealized reaction-zone; symbols are those used in the text.

This is here referred to as the *conservation equation*. The nature of this equation can be visualized by rewriting it,

$$w^B = \frac{d^A w^A a' + d^C w^C (1 - a')}{f d^B} \tag{7}$$

and by introducing the simplifications, $d^A = d^B = d^C$, to give,

$$w^B = [w^A a' + w^C\,(1 - a')]\,/\,f \tag{8}$$

In Figure 5, this equation is plotted for two arbitrary combinations of w^A and w^C. Under these conditions, it is obvious that if $f = 1.0$ and $a' = 0.5$, for example, the concentration (weight fraction) of each conserved element must lie midway between that of A and that of C.

The conservation equation (6) was used to obtain estimates of a' for all elements that were determined in Samples 1 and 2, assuming virtually no change in volume, *i.e.*, $f = 1.0$. Results from Sample 2 are presented as a histogram in Figure 6, and when outliers Cs, Ba, and Rb are excluded, a' (mean) is equal to 0.369, which agrees well with a' (B1–B2 boundary) = 1.20 cm / 3.30 cm = 0.364. For Sample 1, if outliers Cs and Zr are excluded, a' (mean) is equal to 0.172, which agrees well with a' (B1–B2 boundary) = 0.79 cm / 4.31 cm = 0.183. These results are viewed as evidence that most elements were conserved and that the original A–C interface coincided with the present B1–B2 interface.

The observed *variation* in a', *i.e.*, the spread in Figure 6, can be partially understood in relation to the assumption that the composition of the transformed gneiss (C', Fig. 4) was the same as that of gneiss (C) immediately beyond, which was analyzed. The possible effect of inhomogeneity on a' was examined by analyzing four slices of gneiss in Sample 2 (Fig. 2) and by expressing the variation for each element in terms of a very rough standard deviation (S). These S numbers were found to exceed analytical precision (s) by a factor of approximately 8 for major elements and 4 for trace

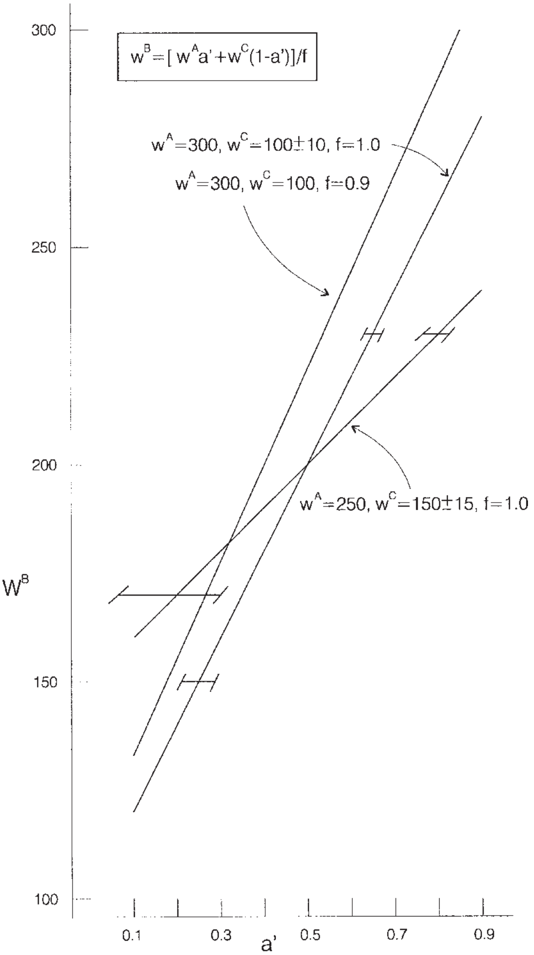

FIG. 5. Plot of equation (8) for arbitrary combinations of w^A and w^C; the effect of a volume change (f = 0.9) is indicated.

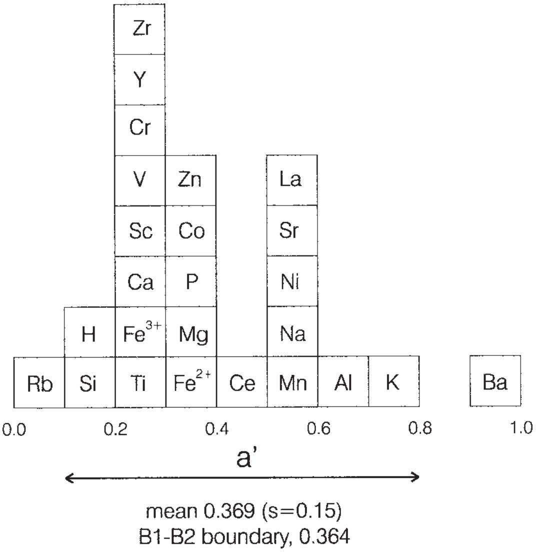

FIG. 6. Values of a' (Sample 2) obtained for various elements by use of the conservation equation (6), assuming no change in volume (f = 1.0). Not shown is outlier Cs (a' = –1.0). Other outliers, Rb and Ba, are excluded in the calculation of mean a' and standard deviation (s).

elements. The result is that inhomogeneity in gneiss can explain some but not all of the departures from a'(mean). For instance, in Sample 2 (Fig. 6), where a' (mean) = 0.37, the uncertainty in a' for Sr (0.53) resulting from inhomogeneity extends from 0.35 to 0.64, and the uncertainty in a' for Rb (0.09) extends from –0.7 to + 0.4. It would be unreasonable, therefore, to conclude that Sr was removed and Rb was added. But for Ba (a' = +1.0), the range is 0.9 to 1.1, and for Cs (a' = –1.0), the range is –1.5 to –0.7; Ba was evidently removed and Cs added. Note that the present method of identifying unconserved elements becomes increasingly ineffective for elements with small A–C differences in concentration.

The principal source of error in *mean a'* for a given sample is the assumption of zero change in volume. Only a small change in volume can cause a large change in a' (calculated) for all conserved elements, as is indicated in Figure 5. But because of the remarkable agreement between a' (mean) and the present position of the B1–B2 interface in both study samples, one must conclude that *changes in volume were very small*. These conditions, 1) present B1–B2 boundary equal to the original A–C boundary, and 2) near-zero change in volume, are here and below referred to as the *boundary proposal*.

Figure 6 identifies a few elements that are suspected of having been added to or removed from a reaction zone, but it lacks information on the magnitude of these changes. Such information is presented in Table 8, where element concentrations in entire reaction-zones, as determined by chemical analysis, can be compared with those expected, on the basis of the boundary proposal, *i.e.*, by use of equation (7), with f = 1.0. The data of Table 8 lead one to suspect that some Ca, K, and Ba were lost, and Cs was added.

THE REACTION

Given the abundant biotite and plagioclase within the reaction zones of Samples 1 and 2 (Fig. 3) and the absence of hornblende and K-feldspar, the (unbalanced) reaction that evidently occurred is: hornblende + K-feldspar → biotite + plagioclase. Mineral compositions (Tables 6, 7) are now used in an attempt to construct a balanced equation representative of the reaction. Coef-

TABLE 8. ELEMENT CONCENTRATIONS IN REACTION ZONES: EXPECTED* AND FOUND

	Sample 1		Sample 2	
	Expected	Found	Expected	Found
Si/wt%	29.8	30.3	28.2	28.8
Ti	0.62	0.59	1.01	0.98
Al	8.41	7.94	7.56	7.83
Fe^{3+}	1.56	1.68	2.93	2.87
Fe^{2+}	3.44	3.27	4.34	4.12
Mn	0.07	0.06	0.09	0.12
Mg	1.51	1.39	1.84	1.63
Ca (-)	2.40	2.19	3.21	2.57
Na	2.55	2.71	1.58	1.34
K (-)	2.84	1.87	2.87	2.13
P/ppm	747	722	1170	1180
Sc	18	13	26	21
V	132	126	228	212
Cr	50	51	63	56
Co	58	54	42	41
Ni	32	29	41	38
Zn	144	174	244	230
Rb	101	118	118	153
Sr	237	241	114	102
Y	38	32	58	52
Zr	253	275	300	293
Cs (+)	2.8	4.4	3.3	7.4
Ba (-)	812	427	800	450
La	27	29	39	33
Ce	58	61	78	76

* Equation (7) and boundary proposal
(-), (+) suspected loss, addition

TABLE 9. BALANCE SHEET, SAMPLE 1, (EQUATION (9))

	Reactants		Products				Sum	
	0.653 Hbl	0.859 Kfs	1.00 Bt	0.320 ab	0.254 an	2.48 Qtz	Reactants	Products
Si	4.15	2.57	2.76	0.96	0.51	2.48	6.72	6.72
Al	1.35	0.86	1.38	0.32	0.51		2.21	2.21
Ti	0.08		0.19				0.08	0.19
Fe^{3+}	0.48	0.01	0.10				0.49	0.10
Fe^{2+}	0.98		0.97				0.98	0.97
Mg	1.38		1.38				1.38	1.38
Mn	0.03		0.02				0.03	0.02
Ca	1.22				0.25		1.22	0.25
Na	0.27	0.06	0.01	0.32			0.33	0.33
K	0.16	0.84	1.00				1.00	1.00
F	0.10		0.14				0.10	0.14
Cl	0.03		0.02				0.03	0.02
OH	1.2		1.8				1.2	1.8

an/(ab + an) = 0.44

ficients are obtained in the usual manner, by solving simultaneous mass-balance equations, one for each element.

The Ca:Al ratio in hornblende in the study samples is close to 1:1, whereas in the anorthite component of plagioclase it is 1:2, and it is therefore not possible to balance both elements simultaneously. By conserving Al, we obtain the following equation for Sample 1,

0.653 hornblende + 0.859 K-feldspar
→ 1.00 biotite + 0.320 albite +
0.254 anorthite + 2.48 quartz, (9)

where biotite refers to that in zone B1. The equation produces plagioclase of composition X_{an} [= Ca/(Ca + Na)] = 0.44, similar to that in zone B1, where X_{an} = 0.40. The balance sheet (Table 9) shows that apart from Ca, balance is obtained for many elements but not for Ti (which was possibly derived from ilmenite), ferric iron (which may indicate that some reduction of iron occurred) and OH (resulting presumably from an introduction of H_2O).

For Sample 2, the equation is,

0.606 hornblende + 0.932 K-feldspar
→ 1.00 biotite + 0.344 albite +
0.291 anorthite + 2.24 quartz; (10)

the balance sheet (Table 10) is similar to that for Sample 1 (Table 9). The possible involvement of garnet (which is present in Sample 2, but not in Sample 1) will be considered below.

Evidence was presented above (Table 8) for minor loss of potassium, which was possibly derived from K-feldspar. Rewriting the equation for Sample 2 by assigning only half of the K to biotite makes more Al available for plagioclase, to yield a ratio X_{an} equal to 0.61 rather than 0.46.

Further information on the reaction can be obtained from variation in the composition of minerals *within* the

TABLE 10. BALANCE SHEET, SAMPLE 2, (EQUATION (10))

	Reactants		Products				Sum	
	0.606 Hbl	0.932 Kfs	1.00 Bt	0.344 ab	0.291 an	2.24 Qtz	Reactants	Products
Si	3.80	2.78	2.73	1.03	0.58	2.24	6.58	6.58
Al	1.39	0.94	1.41	0.34	0.58		2.33	2.33
Ti	0.06		0.19				0.06	0.19
Fe^{3+}	0.35		0.16				0.35	0.16
Fe^{2+}	1.05		0.98				1.05	0.98
Mg	1.25		1.33				1.25	1.33
Mn	0.012		0.004				0.012	0.004
Ca	1.10				0.29		1.10	0.29
Na	0.24	0.12	0.01	0.34			0.35	0.35
K	0.14	0.85	0.99				0.99	0.99
F	0.13		0.21				0.13	0.21
Cl	0.03		0.03				0.03	0.03
OH	1.1		1.8				1.1	1.8

an/(ab + an) = 0.46

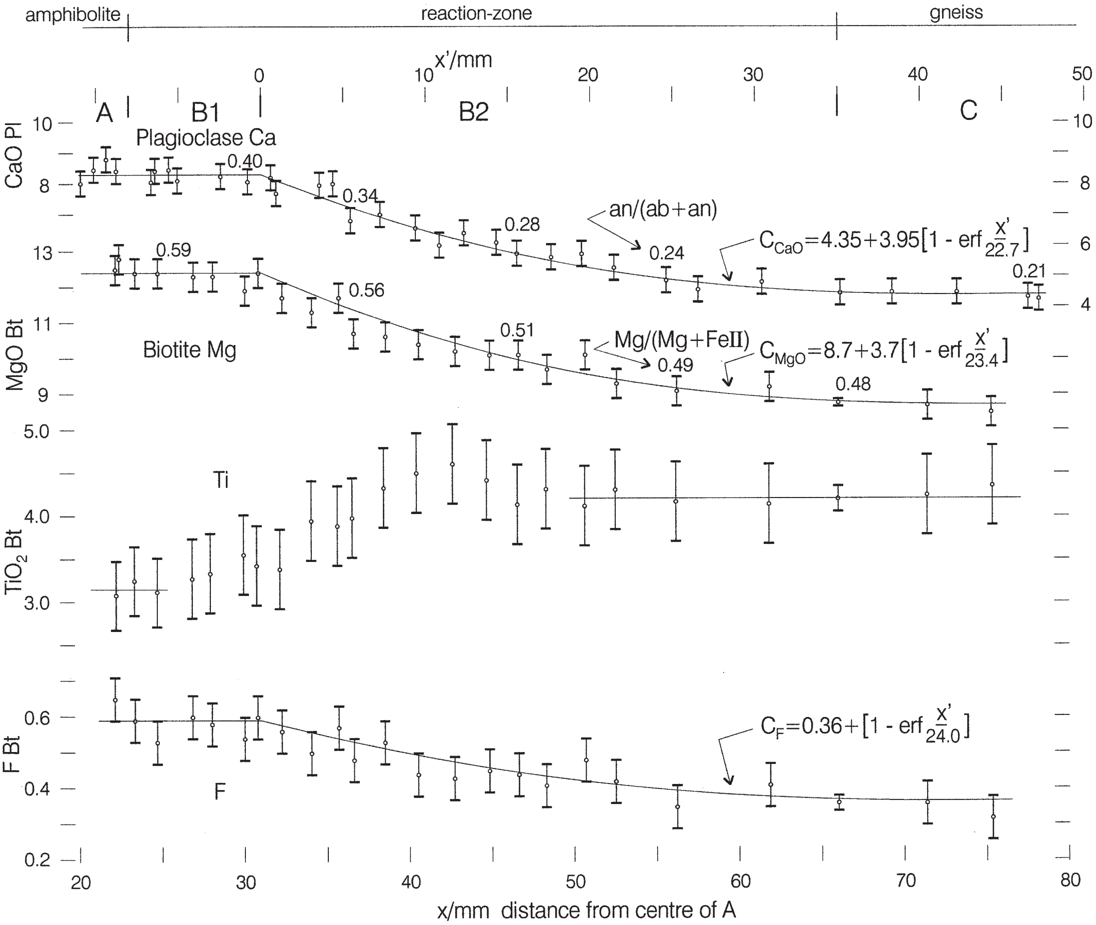

FIG. 7. Variation in the Mg, Ti, and F content of biotite, and in the Ca content of plagioclase in Sample 1. Error-function equations are assigned to the Mg, Ca, and F profiles. The distance from the B1–B2 interface is shown at the top as *x*'. Numbers on the profiles are mole fractions, an/(ab + an) and Mg/(Mg + Fe^{2+}). Error bars define 0.95 confidence limits; at x = 66 mm, small error bars result from ten local determinations of the composition of biotite.

reaction zones. Changes of this kind were first detected by Schrijver (1973) in a granulite terrane north of Montreal.

Variation in the Mg content of biotite in Sample 1, extending from amphibolite (A), across the entire reaction-zone (B) and into gneiss (C), is illustrated in Figure 7. There is a continuous decrease in Mg (increase in Fe^{2+}) from the B1–B2 boundary, through zone B2, extending to C. The variation can be described by use of the equation,

$$C_{MgO} = 8.7 + 3.7\ [1 - \mathrm{erf}\ (x'/23.4)], \qquad (11)$$

where C_{MgO} is wt% MgO in biotite, x' is distance in mm from the B1–B2 interface, and erf stands for the error function. This equation is comparable to the simple equation describing unidirectional diffusion,

$$C = C_0 + C_1\ [1 - \mathrm{erf}\ (x/2\ (D\ t)^{1/2})], \qquad (12)$$

where C is the concentration of diffusing atoms within a phase in which the initial concentration is C_0, expressed as a function of distance, x, from a boundary where concentration is constant at C_1; D is the diffusion coefficient and t is elapsed time (Shewmon 1963). The overall decrease in Mg corresponds to a change in X_{Mg} [= Mg/(Mg + Fe^{2+})] from 0.59 (in amphibolite and the biotite-rich zone, B1) to 0.48 (in gneiss) (Fig. 7). A decrease in the fluorine content of biotite also has been detected; it can be described by

$$C_F = 0.36 + 0.23\ [1 - \mathrm{erf}\ (x'/24.0)] \qquad (13)$$

The variation in Ti (Fig. 7) is more irregular.

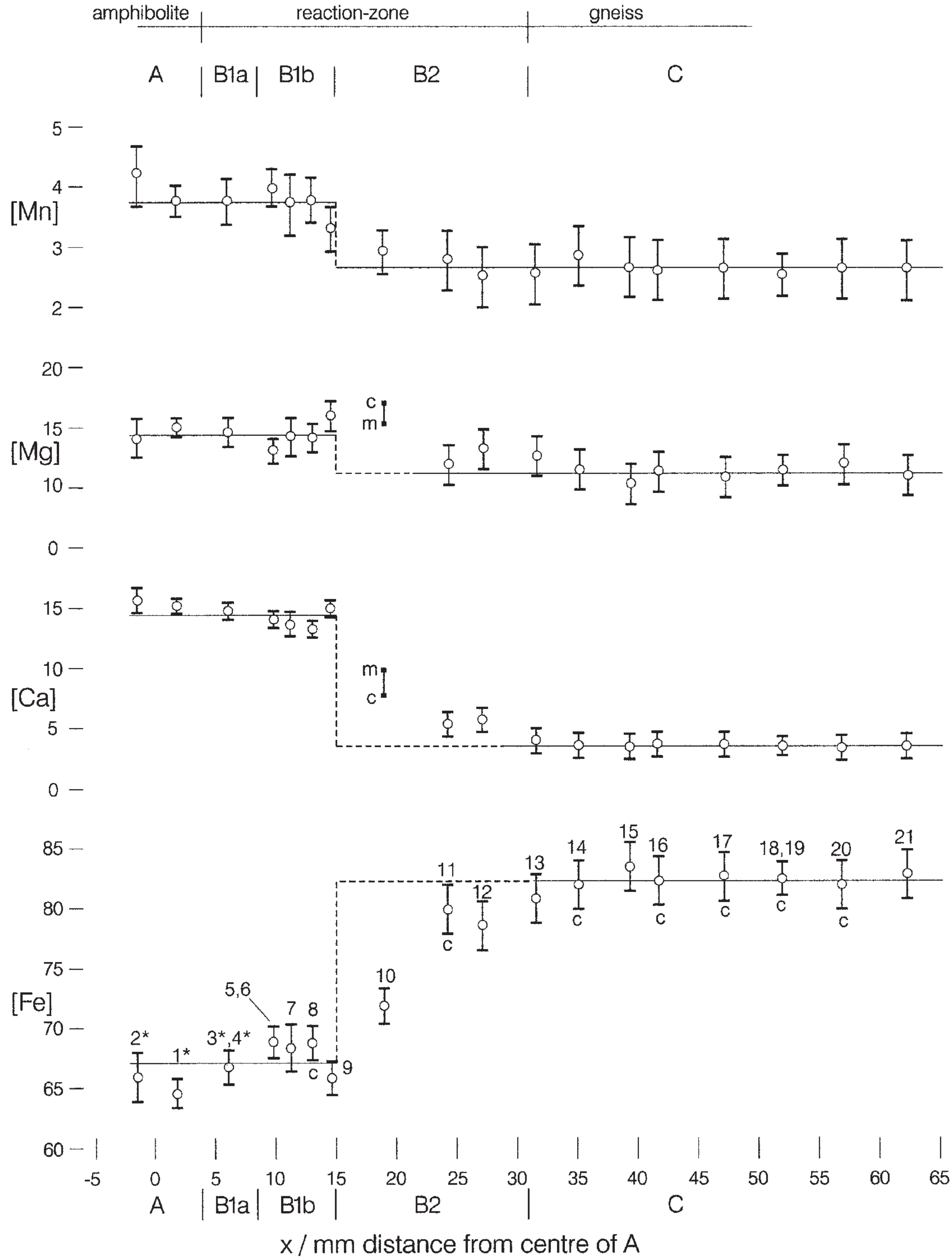

FIG. 8. Variation in the composition of garnet in Sample 2. Crystals are numbered on the [Fe] profile; c refers to crystal centers (as seen in section); remainder are margins. Large center (c) – margin (m) differences occur only in crystal 10 ([Ca] and [Mg]). Crystals 1 to 4 have many inclusions of ilmenite. Concentrations are expressed in mole %, *e.g.*, 100 Fe/(Fe + Mg + Mn + Ca). Error bars are estimates of uncertainty based on replicate analyses of the margin.

A similar progression exists in the Ca content of associated plagioclase (Fig. 7), for which the equation is

$$C_{\mathrm{CaO}} = 4.35 + 3.95\,[1 - \mathrm{erf}\,(x'/22.7)], \qquad (14)$$

corresponding to a decrease in X_{an} from 0.40 to 0.21 (Fig. 7). Note that the denominator in the last term of equations (11), (13), and (14) is nearly the same, as it must be if variations in concentration are confined to a zone of given width.

In Sample 2, the Mg content of biotite decreases in a step-wise manner from amphibolite to the B1–B2 boundary (Table 7), and beyond this boundary, it decreases continuously as in Sample 1, following the relation

$$C_{\mathrm{MgO}} = 6.49 + 5.41\,[1 - \mathrm{erf}\,(x'/14.2)]. \qquad (15)$$

The decrease extends somewhat into gneiss. Variation in the Ca content of plagioclase in zone B2 is more irregular than in Sample 1, but follows approximately the relation

$$C_{\mathrm{CaO}} = 5.1 + 12.5\,[1 - \mathrm{erf}\,(x'/6.82)]. \qquad (16)$$

The shape of the fluorine-in-biotite profile is much like that in Sample 1:

$$C_{\mathrm{F}} = 0.40 + 0.51\,[1 - \mathrm{erf}\,(x'/13.5)] \qquad (17)$$

A relatively "steep" gradient in Ca results in a relatively small denominator (6.82) in equation (16).

Although the concentration profiles described above [equations (11) and (13) to (17)] possibly began to form prior to the time during which the reaction zones were created, or afterward, the preferred interpretation is that they formed while the hornblende + K-feldspar → biotite + plagioclase reaction was in progress, and that they must be explained in terms of the re-arrangement of atoms that occurred at that time.

Garnet (not present in Sample 1) occurs in all zones of Sample 2 (Table 2, Fig. 3). The abundant garnet in the reaction zone of sample 2 creates the impression that this mineral is a product of the reaction, but in view of the Ca–Al problem, described above, it is virtually impossible to bring garnet into the reaction [equation (10)] unless one assumes that Al was introduced. Garnet in Sample 2 is very irregularly distributed, and this presumably explains its large modal abundance in zone B1b. Nor is there any modal or microstructural evidence that garnet was consumed.

Suppose therefore that garnet remained entirely passive as reaction occurred. Then in view of the boundary proposal, stated above, garnet crystals in zones B1a and B1b should have the same composition as those in amphibolite (A), and from Table 7 and Figure 8, they appear to do so. Also, crystals in B2 should have the same composition as those in gneiss (C), but certainly crystal 10, and possibly also crystals 11 and 12 (Fig. 8), contain more Mg and Ca, and less Fe, than those in adjacent gneiss.

Additional information was obtained from Sample 3, which is shown in Figure 9a. Compositions of garnet crystals 1 to 6 and of biotite crystals in the vicinity of each appear in Table 11; variation in Ca is also shown in Figure 9b.

With regard to zones B1a and B1b, Table 11 confirms the findings from Sample 2, that garnet crystals in A, B1a and B1b are nearly identical in composition, as expected if these zones were initially amphibolite, and little change in garnet composition occurred subsequently. Moreover, ilmenite inclusions, which characterize garnet in amphibolite, also are present in zone B1a; why they are not present in crystal 3, within zone B1b, is not known.

Information on the distribution of Mg and Fe^{2+} among crystals 1 (in A), 2 (in B1a), 3 (in B1b) and associated biotite is presented in Table 11, in the form of a distribution coefficient, defined as

$$K_{\mathrm{D}} = \frac{X_{\mathrm{Mg}}{}^{\mathrm{Bt}}\,(1 - X_{\mathrm{Mg}}{}^{\mathrm{Grt}})}{(1 - X_{\mathrm{Mg}}{}^{\mathrm{Bt}})\,X_{\mathrm{Mg}}{}^{\mathrm{Grt}}} \qquad (18)$$

where $X_{\mathrm{Mg}} = \mathrm{Mg} / (\mathrm{Mg} + \mathrm{Fe}^{2+})$, and also in Figure 10. A nearly constant distribution-coefficient, as well as a temperature estimate of approximately 690°C, obtained by use of the relation,

$$\mathrm{T} = \frac{2780 - 258\,[\mathrm{Ca}]}{\ln K_{\mathrm{D}} + 0.235\,[\mathrm{Ca}] + 1.51} \qquad (19)$$

from Kretz (1994b, p. 228), which agrees with other temperature estimates in the study area, both provide evidence for the preservation of Mg– Fe exchange equilibrium in zones A, B1a and B1b as reaction progressed.

TABLE 11. MARGINAL COMPOSITION* OF GARNET CRYSTALS IN SAMPLE 3 AND Mg-Fe DISTRIBUTION BETWEEN MARGINS AND ASSOCIATED BIOTITE

Crystal	Zone	[Fe]		[Mg]		[Mn]	[Ca]		$X_{\mathrm{Mg}}^{\mathrm{Grt}}$	$X_{\mathrm{Mg}}^{\mathrm{Bt}}$	K_{D}	T**
1	A	64.6		16.0		4.1	15.3		0.199	0.632	6.9	680
2	B1a	66.0		14.5		4.2	15.1		0.180	0.579	6.3	700
3	B1b	64.6		15.2		4.2	16.0		0.190	0.609	6.6	690
4	B2	71.6		15.9	(18.5)	3.8	8.9	(5.9)	0.182	0.530	5.1	700
5	B2	78.8	(76.5)	13.2	(13.6)	2.5	5.5	(7.9)	0.143	0.417	4.3	710
6	C	81.1	(77.3)	11.8	(12.3)	2.5	4.6	(8.4)	0.127	0.361	3.9	730

* and in parentheses, central composition, where different from that in margins. [Fe] etc. are molar fractions, 100Fe/(Mg + Fe + Mn + Ca) etc. $X_{\mathrm{Mg}} = \mathrm{Mg}/(\mathrm{Mg}+\mathrm{Fe}^{2+})$

** $\mathrm{T} = [(2780 - 258\,[\mathrm{Ca}]) / (\ln K_{\mathrm{D}} + 0.235\,[\mathrm{Ca}] + 1.51)] - 273$

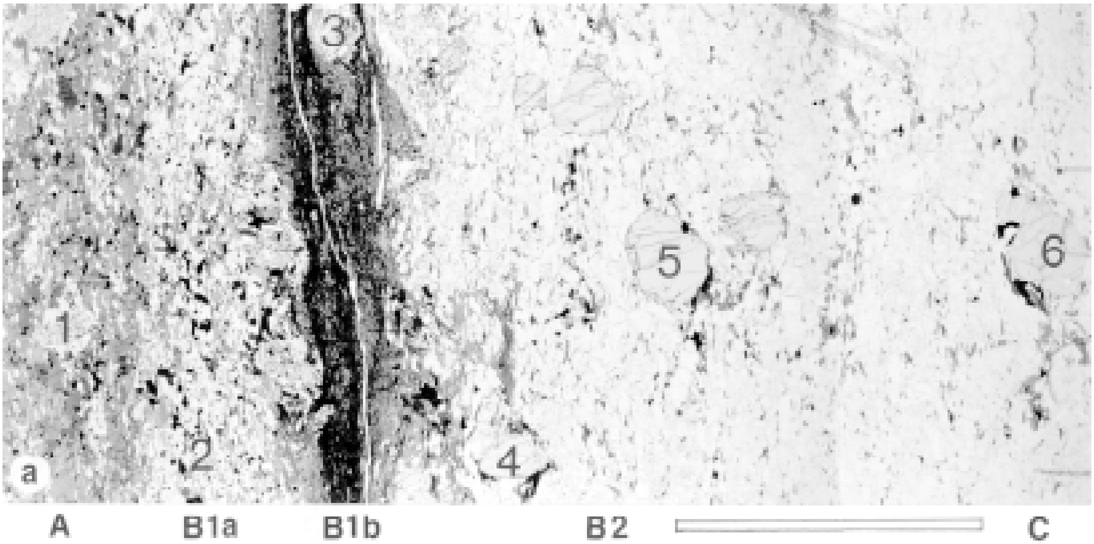

FIG. 9. (a) Sample 3, (bar: 1.0 cm), and (b) spot concentrations expressed as 100 Ca/(Fe + Mg + Mn + Ca) in garnet crystals numbered 1 to 6 in (a); concentration numbers lie immediately above points chosen for characterization by electron-microprobe analyses. Bar in (b): 1.0 mm.

Moving now into zone B2, some new compositions of garnet are encountered. It is instructive to enter zone B2 from the gneiss (C), where conspicuous zoning appears in crystal 6; this, being a large crystal, was presumably cut nearly through the center. Here, Fe increases from center to margin, whereas Ca decreases (Fig. 9b), as Mg possibly decreases slightly and Mn remains unchanged (Table 11). Crystal 6 was presumably unaffected by the formation of the reaction zone.

Comparing crystal 5, in the outer part of zone B2, with crystal 6, the margin is distinctly higher in Ca and Mg content, and lower in Fe than is the margin of 6; a migration of Ca and Mg atoms into this crystal, in exchange for Fe, has evidently occurred. Moving to crystal 4 in the inner part of zone B2, a further and more conspicuous increase in Ca and Mg, accompanied by a decrease in Fe, are observed, and the level of Mn has evidently also increased (Table 11). Compared with crystals 6 and 5, the rather large apparent addition of Ca to the margin of crystal 4 has resulted in a reversal in the zoning profile (Fig. 9b).

Information on the distribution of Mg and Fe between the margins (outer 0.5 mm) of crystals 6, 5, and 4, and associated crystals of biotite, appears in Table 11 and Figure 10. In Figure 10, the broken-line arrow expresses the progressive increase in Mg and Ca within garnet margins, in exchange for Fe, extending from the B2–C boundary to the B1–B2 boundary. What is especially noteworthy is that Mg–Fe exchange equilibrium (garnet margins – biotite) was maintained as the biotite-forming reaction progressed, with the distribution coefficient faithfully changing in response to the Ca content of garnet, as demanded by equation (19), at a temperature of approximately 700°C (Table 11).

In summary, garnet in Samples 2 and 3 was neither a reactant nor a product, and was involved only in that crystal margins in zone B2 adsorbed some Ca and Mg atoms and released an equal number of Fe atoms.

SPATIAL DISTRIBUTION OF REACTION PRODUCTS

Reaction zones of the present study are far from homogeneous. Most conspicuous (Tables 1 and 2, Fig. 3) is the abundance of biotite in subzone B1 relative to B2 (by a factor of 4 to 7) and of plagioclase in B2 relative to B1 (by a factor of 1.6). Nearly all major and trace elements are concentrated either in B1 or B2.

In view of the boundary proposal, as stated above, and the finding that A–B1 and C–B2 density contrasts (Tables 1 and 2) are small (<4% and <2%, respectively), it is now permissible to compare element concentrations (wt% or ppm) in A and B1 and in C and B2 *directly*, without recourse to the Gresens (1967) equation. Carrying out the comparisons (Tables 4 and 5), taking into consideration analytical imprecision and local variability, it is apparent that for many elements, concentrations in zone B1 are indistinguishable from those in adjacent amphibolite (A), and similarly those in B2 are indistinguishable from those in adjacent gneiss (C). It is possible, then, to group the elements as follows.

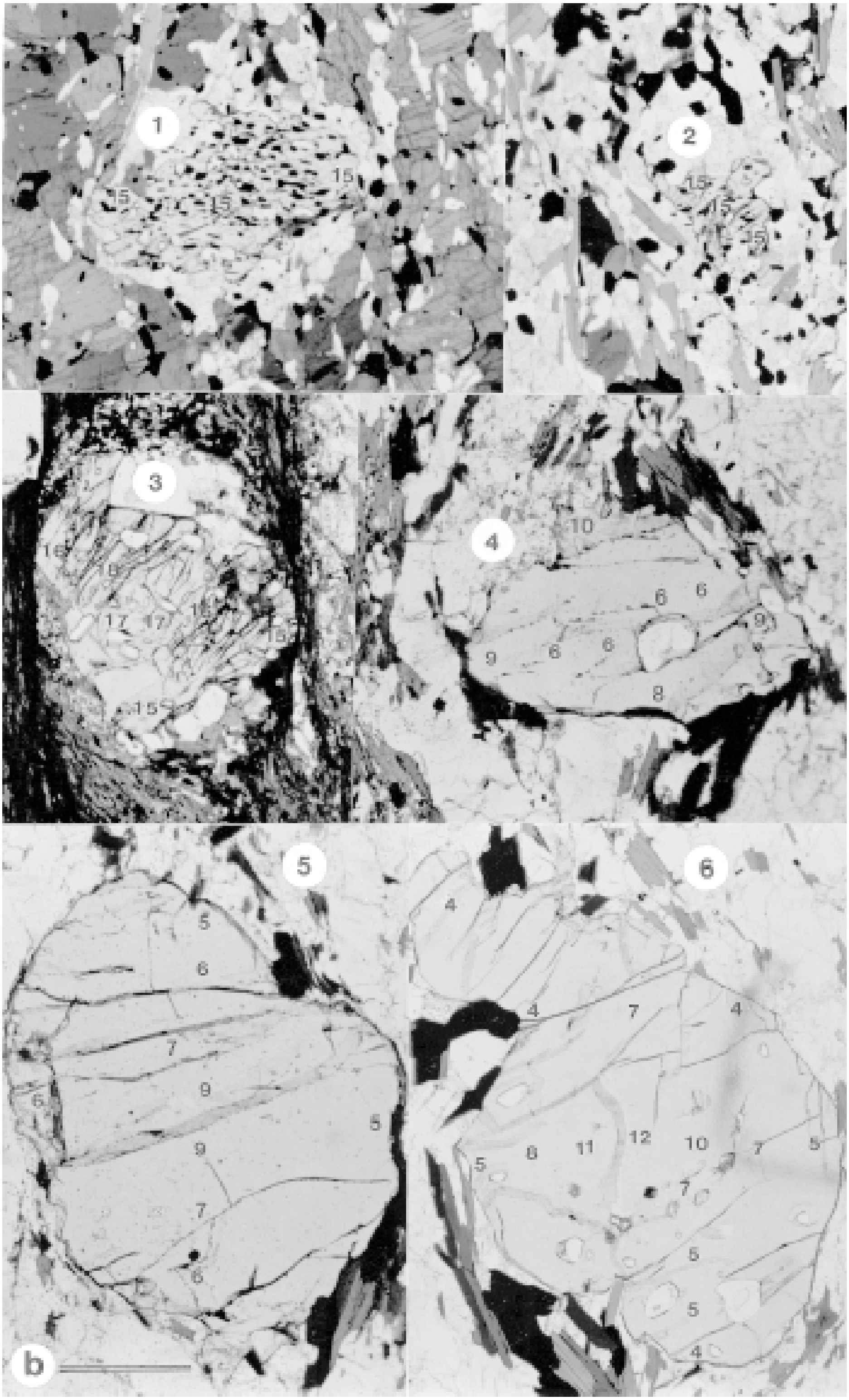
1
15
15
15
2
15
15
15
3
16
17
17
15
15
4
10
6
6
9
9
6
6
8
5
5
6
7
9
9
5
7
6
6
4
4
7
4
5
8
11
12
10
7
5
7
5
5
4
b

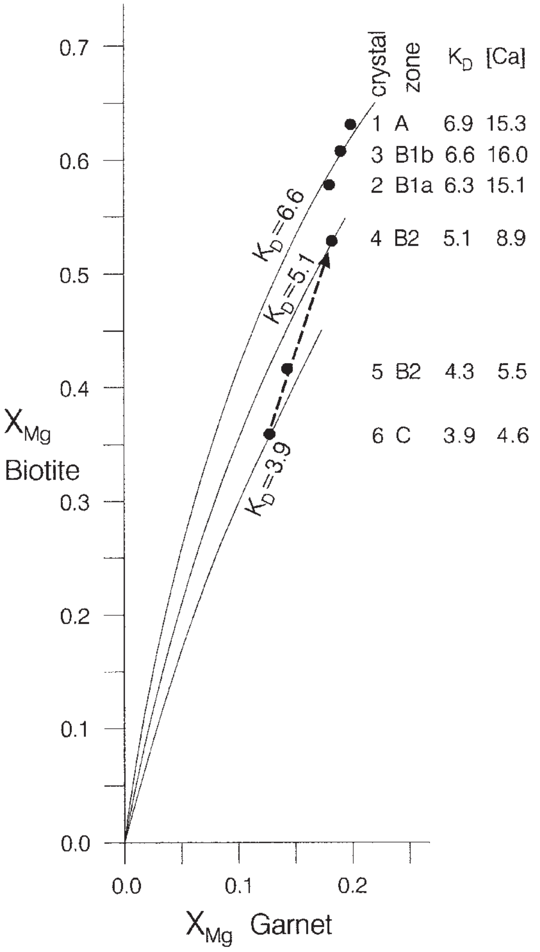

FIG. 10. Distribution of Mg and Fe^{2+} between garnet (margins) and biotite in Sample 3 (Fig. 9). K_D is the distribution coefficient (equation 18). The arrow represents a change across zone B2 from gneiss to the B1–B2 boundary.

In place

I	(A > C): B1 = A, B2 = C	Ti Fe Mn Mg P Sc V Cr Co Ni Zn
II	(C > A): B1 = A, B2 = C	Si Sr Zr La Ce
III	A ~ B1 ~ B2 ~ C	Al Y

Displaced

IV	(A > C): B2 > B1	Ca (Mg)	from A to B2
V	(C > A): B2 > B1	Na	from A to B2
VI	(C > A): B1 > B2	K Rb Ba	from C to B1

Elements of group I are more abundant in amphibolite than in gneiss (A > C), and using the criteria cited above, concentrations in amphibolite and adjacent B1 are indistinguishable (B1 = A), as are concentrations in gneiss and adjacent B2 (B2 = C). Elements of group II are more abundant in gneiss than in amphibolite (C > A), and similarly, the relationships B1 = A and B2 = C apply. Elements of group III differ only slightly throughout. Elements of these three groups have therefore remained largely, through not necessarily entirely, in place during reaction-zone formation. Note that several group-I elements resided in hornblende, and as these crystals broke down, the elements entered newly crystallizing biotite in the vicinity.

Of special interest are the displaced elements of groups IV to VI. Calcium is more abundant in amphibolite than in gneiss but now is concentrated in B2, adjacent to gneiss; thus Ca atoms must have migrated from hornblende at the A–B1 boundary, across the entire reaction-zone, to crystallizing plagioclase at the B2–C boundary. Sodium, although more abundant in C than in A, followed Ca. Potassium, Rb, and Ba, which were released from K-feldspar, must have migrated in the opposite direction, to enter crystallizing biotite in B1. Similar displacements for calcium and potassium were detected by Ono (1977) and Owen (1993).

Given the above information and an equation for the entire reaction in Sample 1 (Table 9), half reactions that occurred on either side of the reaction zone can be proposed. At the A–B1 boundary:

$$\begin{aligned}&0.65\ \text{hornblende} + (0.84\ \text{K})\\&\rightarrow 1.00\ \text{biotite} + 1.4\ \text{quartz} +\\&(0.25\ \text{Ca} + 0.26\ \text{Na}) + [0.97\text{Ca}]\end{aligned}\tag{20}$$

At the C–B2 boundary:

$$\begin{aligned}&0.86\ \text{K-feldspar} + (0.25\ \text{Ca} + 0.26\ \text{Na})\\&\rightarrow 0.32\ \text{albite} + 0.25\ \text{anorthite} +\\&1.1\ \text{quartz} + (0.84\ \text{K})\end{aligned}\tag{21}$$

In parentheses are atoms that arrived from the opposite boundary of the entire reaction-zone, and in square brackets, the Ca that was evidently lost to the surroundings. Half reactions for Sample 2 are similar to (20) and (21).

In addition to the changes expressed by these equations, a small fraction of the total Mg released from hornblende crossed the B1–B2 boundary and entered pre-existing biotite crystals, in exchange for Fe^{2+}, accompanied by minor Ti and F (Fig. 7). Similarly, minor Ca evidently also crossed this boundary and (together with locally derived Al) entered pre-existing plagioclase crystals by way of $CaAl \rightleftharpoons Na\,Si$ exchange. In sample 2, minor Ca and Mg evidently entered margins of garnet crystals in B2, in exchange for Fe.

Although minerals were not analyzed for Rb and Ba, elsewhere in the study area, these elements are concentrated in K-feldspar and biotite relative to plagioclase, according to the following distribution-formulas: Rb: Bt 2.3 Kfs 23 Pl; Ba: Kfs 4.0 Bt 12 Pl (Kretz *et al.* 1999), *i.e.*, the two elements are concentrated in K-feldspar relative to plagioclase by factors of 23 for Rb and 48 for Ba. Thus, when released from K-feldspar, these atoms were "reluctant" to enter newly crystallizing plagioclase, and presumably followed potassium to enter newly crystallizing biotite, in an attempt to establish exchange equilibrium between biotite and plagioclase. *Note that the three elements that were most "mobile" within the reaction zones* (*Ca, K, Ba*) *are the very elements for which evidence was found* (*Table 8*) *for a partial loss from the reaction zones*.

Why biotite crystallized near hornblende and plagioclase near K-feldspar rather than *vice versa* will now be considered briefly in terms of volume change.

By use of molar volume data for minerals of simplified formulas, as compiled by Robie *et al.* (1979), an estimate may be obtained for the volume change for the biotite–plagioclase-forming reaction [equations (9) and (10), Tables 9 and 10] as follows:

	hornblende +	K-feldspar →	biotite
1:	178	93	150
2:	165	101	150

	+ plagioclase	+ quartz	
1:	58	56	$\Delta V = -2.8\%$
2:	64	51	$\Delta V = -0.5\%$

Here, 1 and 2 refer to Samples 1 and 2, and the numbers are in units of cm^3 relative to 1 mole of biotite. Because hornblende and biotite volumes are similar, micro changes in volume are expected to be more readily accommodated when biotite crystallizes in the vicinity of hornblende rather than K-feldspar, and the observed distribution of minerals appears to be energetically favorable relative to other possible distributions.

Moreover, the observed distribution of crystals is certainly the most efficient one with regard to the displacement of atoms. The crystallization of biotite adjacent to amphibolite and plagioclase adjacent to gneiss, with quartz crystallizing at both places, requires a transport of only a few elements across the reaction zones, *i.e.*, the half reactions are simple. As an alternative, the crystallization of biotite adjacent to gneiss would require a complex flux of many elements through the reaction zones.

DISCUSSION

Mineral stability

In various gneisses of the study area, hornblende and K-feldspar occur together commonly, implying that they form a stable association. Why then, at boundaries between amphibolite and gneiss, did they break down [equations (9) and (10)] to form biotite and plagioclase? Two possibilities will be considered. One is that a stable hornblende – K-feldspar association can be made unstable by shear stress, as proposed in general terms by Harker (1932, p. 150). With the amphibolite layers behaving as relatively rigid bodies, a shear stress is expected to develop at the boundaries with gneiss during deformation, as well as a concentration of strain, for which evidence exists in the pronounced biotite foliation in subzone B1. Hornblende is known to be "exceedingly strong" (Morrison-Smith 1976), whereas biotite is "weak in shear" (Christoffersen & Kronenberg 1993), and the high strain-energy of hornblende crystals subjected to shear, resulting in a high density of dislocations, could conceivably have caused the energy of hornblende + K-feldspar [the left-hand side of (9) and (10)] to exceed that of biotite + plagioclase (the right-hand side). An analogy is the crystallization of aragonite from strained calcite, described by Newton *et al.* (1969).

Alternatively, in view of the finding that hydrogen was added and calcium was removed (Tables 9, 10), an explanation might be sought in terms of a high activity of hydrogen (or H_2O) and a low activity of calcium at contacts between amphibolite and gneiss.

Diffusion

The importance of diffusion as a mechanism for the transport of atoms and molecules during metamorphism was emphasized by Ramberg (1952) and has been considered in some detail by Mueller (1967), Frantz & Mao (1979), Brady (1983), Joesten (1991) and others.

For changes that have occurred on a very small scale (*e.g.*, exsolution), it seems certain that individual atoms were displaced through crystals, but on the scale of a few cm, crystal-boundary diffusion is frequently called on as the principal mechanism of transport. The difficulty in dealing with crystal-boundary diffusion is that the nature of the diffusing particles and the composition and structure of the crystal-boundary phase are not known.

Direct evidence for diffusion over a distance of a few cm or more can be found in places where variations in mineral abundance or composition can be described by use of diffusion equations. Such changes have possibly resulted from the diffusion of certain atoms along crystal boundaries, accompanied by the immobilization of some of the atoms as they enter crystals along the way. The theory was treated by Crank (1975) and was applied by the writer (1994b, p. 438) to the crystallization of tourmaline resulting from the diffusion and partial immobilization of boron. Applying the same reasoning to the observed changes in the composition of biotite in zone B2 of Sample 1 (Fig. 7), let C_1 represent a constant concentration of Mg in the crystal-boundary phase at the B1–B2 interface, C, the concentration of Mg in this phase at a distance x' from the interface, s the fraction of Mg immobilized (by entering biotite) at any point along x', D the crystal-boundary diffusion coefficient for the Mg particles, and t the elapsed time; moreover, let s/C, denoted R, remain constant. Then the appropriate equation expressing a relation between s (decrease in Mg content of biotite) and distance x' from the B1–B2 interface is

$$s = RC_1\left[1 - \operatorname{erf}\left\{\frac{x'}{2\left(D/\left(R+1\right)\right)^{1/2} t^{1/2}}\right\}\right] \quad (22)$$

This, being the form of the relations [equations (11) to (17)] that were found for Mg and F in biotite and Ca in plagioclase, is here viewed as evidence that the movement of Mg, Ca, and F into zone B2 occurred principally by crystal-boundary diffusion.

Liu & Yund (1992) have studied CaAl – NaSi exchange diffusion in plagioclase; if one extrapolates their results to 700°C, the diffusion coefficient (D) is approximately 1×10^{-20} cm^2s^{-1}, which yields a calculated mean displacement $\bar{x} = (Dt)^{1/2}$ of 0.1 mm for a time (t) of 100 M.y. With plagioclase crystals 1 to 1.5 mm in diameter, and a general absence of compositional zoning, either the diffusion coefficient is too small, or the time estimate is too short, or possibly dynamic recrystallization occurred to assist in producing homogeneous crystals.

The observed changes in the margins of garnet crystals in zone B2 of Samples 2 and 3 (increase in Ca and Mg; decrease in Fe) presumably also occurred by diffusion, *i.e.*, Ca–Fe and Mg–Fe exchange diffusion in garnet. Schwandt *et al.* (1996) have measured self-diffusion of Ca in grossular; assuming that D for Ca self-diffusion and Ca–Fe exchange diffusion are nearly equal, a calculation of mean displacement (as above) gives $\bar{x} = 0.2$ mm, which is consistent with Ca having invaded the margins of the crystals, but not the interiors.

With regard to the migration of Ca, Na, K, Rb, and Ba across the reaction zones, the finding that different kinds of atoms have moved in opposite directions also is consistent with diffusion rather than some other mechanism of transport.

It is important to recognize that diffusion is a random process that is better described by use of the term "drift" rather than "flow". Thus at least a small proportion of the Ca atoms released by hornblende must have been displaced in the direction of amphibolite, and some potassium released from K-feldspar must have moved into gneiss. This may explain the above-reported loss of some atoms of these elements from the volumes now occupied by the reaction zones.

CONCLUSION

In the Otter Lake area, the formation of mineral zones at boundaries between amphibolite and gneiss was examined in relation to a gain or loss of elements from and to the surroundings. An examination of bulk compositions, making use of a newly derived equation to express conservation, led to the conclusion that 1) the present boundary between the two principal subzones (one rich in biotite and the other with abundant plagioclase) coincides with the original amphibolite–gneiss interface, and 2) only four of 25 elements were not conserved, these being Ca, K, and Ba (removed) and Cs (added).

By use of mineral compositions, it was possible to construct a reaction equation, hornblende + K-feldspar → biotite + plagioclase + quartz, that is balanced or nearly balanced for major elements except Ca, in agreement with the finding that some Ca was lost. In detail, the reaction was complex because it caused changes to occur in the composition of pre-existing biotite, plagioclase, and garnet, which can be seen as attempts to achieve Mg–Fe exchange equilibrium and phase homogeneity within the reaction zones.

An examination of the distribution of elements within the reaction zones, by use of chemical compositions of subzones, led to the conclusion that most of the major and trace elements remained largely in place, and that the principal across-reaction-zone migrations were those of Ca and Na, toward gneiss, to enter crystallizing plagioclase, and of K, Ba and Rb toward amphibolite, to enter crystallizing biotite. Thus elements that were most mobile within reaction zones (notably Ca, K, Ba) are the same elements that were lost from the reaction zones.

Diffusion equations provide a satisfactory description of variation in the composition of biotite and plagioclase within the reaction zones, and evidently both crystal-boundary and within-crystal diffusion were the principal mechanisms of atomic re-arrangement during reaction-zone formation.

The cause for the nucleation and growth of biotite near crystals of hornblende, and of plagioclase near K-feldspar, rather than *vice versa*, was considered briefly in terms of changes in volume on a small scale. An outstanding problem is the cause for the destabilization of hornblende and K-feldspar, which was here examined tentatively in terms of strain energy.

ACKNOWLEDGEMENTS

This study was supported by the Natural Sciences and Engineering Research Council of Canada. The assistance of Sylvie Thériault, Natalie Morisset, R. Hartree, G. Poirier, E. Hearn, and G. Mrazek is greatly appreciated. Comments from R.F. Martin, T. Rivers, and an anonymous reviewer were very helpful.

REFERENCES

BRADY, J.B. (1983): Intergranular diffusion in metamorphic rocks. *Am. J. Sci.* **283-A**, 181-200.

CHAYES, F. (1956): *Petrographic Modal Analysis*. John Wiley & Sons, New York, N.Y.

CHRISTOFFERSEN, R. & KRONENBERG, A.K. (1993): Dislocation interactions in experimentally deformed biotite. *J. Struct. Geol.* **15**, 1077-1095.

CRANK, J. (1975): *The Mathematics of Diffusion*. Clarendon Press, Oxford, U.K.

FRANTZ, J.D. & MAO, H.K. (1979): Bimetasomatism resulting from intergranular diffusion. II. Prediction of multimineralic zone sequences. *Am. J. Sci.* **279**, 302-323.

GRESENS, R.L. (1967): Composition–volume relations in metasomatism. *Chem. Geol.* **2**, 47-65.

HARKER, A. (1932): *Metamorphism.* E.P. Dutton & Co., New York, N.Y.

JOESTEN, R. (1991): Grain-boundary diffusion kinetics in silicate and oxide minerals. *Adv. Phys. Geochem.* **8**, 345-395.

KRETZ, R. (1978): Distribution of Mg, Fe^{2+} and Mn in some calcic pyroxene – hornblende – biotite – garnet gneisses and amphibolites from the Grenville Province. *J. Geol.* **86**, 599-619.

________ (1980): Occurrence, mineral chemistry, and metamorphism of Precambrian carbonate rocks in a portion of the Grenville Province. *J. Petrol.* **21**, 573-620.

________ (1988): SEM study of dolomite microcrystals in Grenville marble. *Am. Mineral.* **73**, 619-631.

________ (1990): Biotite and garnet compositional variation and mineral equilibria in Grenville gneisses of the Otter Lake area, Quebec. *J. Metamorph. Geol.* **8**, 493-506.

________ (1994a): Petrology of veined gneisses of the Otter complex, southern Grenville Province. *Can. J. Earth Sci.* **31**, 835-851.

________ (1994b): *Metamorphic Crystallization.* John Wiley & Sons, Chichester, U.K.

________ (1997): Metamorphic crystallization: examples from the Ottawa Valley and Laurentian Highlands. *Geol. Assoc. Can. – Mineral. Assoc. Can., Guidebook, Field Trip* **A6**.

________, CAMPBELL, J.L., HOFFMAN, E.L., HARTREE, R. & TEESDALE, J. (1999): Approaches to equilibrium in the distribution of trace elements among the principal minerals in a high-grade metamorphic terrane. *J. Metamorph. Geol.* **17**, 41-59.

________ & HARTREE, R. (1998): Use of parabolic equations to relate standard deviation and concentration in XRF (fused disc) determinations of major and trace elements in silicate rocks. Unpubl. Rep.

________, JONES, P. & HARTREE, R. (1989): Grenville metagabbro complexes of the Otter Lake area, Quebec. *Can. J. Earth Sci.* **26**, 215-230.

LIU, M. & YUND, R.A. (1992): NaSi–CaAl interdiffusion in plagioclase. *Am. Mineral.* **77**, 275- 283.

MORRISON-SMITH, D.J. (1976): Transmission electron microscopy of experimentally deformed hornblende. *Am. Mineral.* **61**, 272-280.

MUELLER, R.F. (1967): Mobility of elements in metamorphism. *J. Geol.* **75**, 565-582.

NEWTON, R.C., GOLDSMITH, J.R. & SMITH, J.V. (1969): Aragonite crystallization from strained calcite at reduced pressures and its bearing on aragonite in low-grade metamorphism. *Contrib. Mineral. Petrol.* **22**, 335-348.

ONO, A. (1977): Chemical reactions at the boundary between gneiss and amphibolite in the Ryoke metamorphic terrain at Takato, Japan. *J. Geol. Soc. Japan* **83**, 33-40.

OWEN, J.V. (1993): Syn-metamorphic element transfer across lithological boundaries in the Port-aux-Basques gneiss complex, Newfoundland. *Lithos* **29**, 217-233.

POTTS, P.J., TINDLE, A.G. & ISAACS, M.C. (1983): On the precision of electron microprobe data: a new test for the homogeneity of mineral standards. *Am. Mineral.* **68**, 1237-1242.

RAMBERG, H. (1952): *The Origin of Metamorphic and Metasomatic Rocks.* University of Chicago Press, Chicago, Illinois.

RIVERS, T. (1997): Lithotectonic elements of the Grenville Province; review and tectonic implications. *Precamb. Res.* **86**, 117-154.

ROBIE, R.A., HEMINGWAY, B.S. & FISHER, J.R. (1979): Thermodynamic properties of minerals and related substances at 298.15 K and 1 bar (10^5 Pascals) pressure and at higher temperatures. *U.S. Geol. Surv., Bull.* **1452**.

SCHRIJVER, K. (1973): Bimetasomatic plagioclase–pyroxene reaction zones in granulite facies. *Neues Jahrb. Mineral., Abh.* **119**, 1-19.

SCHWANDT, C.S., CYGAN, R.T. & WESTRICH, H.R. (1996): Ca self-diffusion in grossular garnet. *Am. Mineral.* **81**, 448-451.

SHEWMON, P.G. (1963): *Diffusion in Solids.* McGraw-Hill, New York, N.Y.

TUISKU, P. (1992): Contact zone interaction of metabasites with metapelites: amphibolite facies mineral assemblages, chemical profiles and their origin, the Puolankajärvi Formation, Finland. *Lithos* **27**, 279-300.

Received July 26, 1999, revised manuscript accepted May 10, 2000.